MPAS-seaice: A new variable resolution sea-ice model

Adrian K. Turner, William H. Lipscomb and Elizabeth C. Hunke

Los Alamos National Laboratory

LA-UR-15-29272

NG23A-1780

Introduction

- We have developed a new global sea-ice model that uses a variable resolution mesh.
- The model uses the Modeling for Prediction Across Scales (MPAS) framework [1].
- It is designed to reproduce the results of Los Alamos' previous sea-ice model, CICE.

MPAS grids

- MPAS grids are Spherical Centroidal Voronoi Tesselations (SCVTs).
- These grids allow regions of the domain to have increased resolution with a smooth transition region between high and low resolution regions (see figure 1).

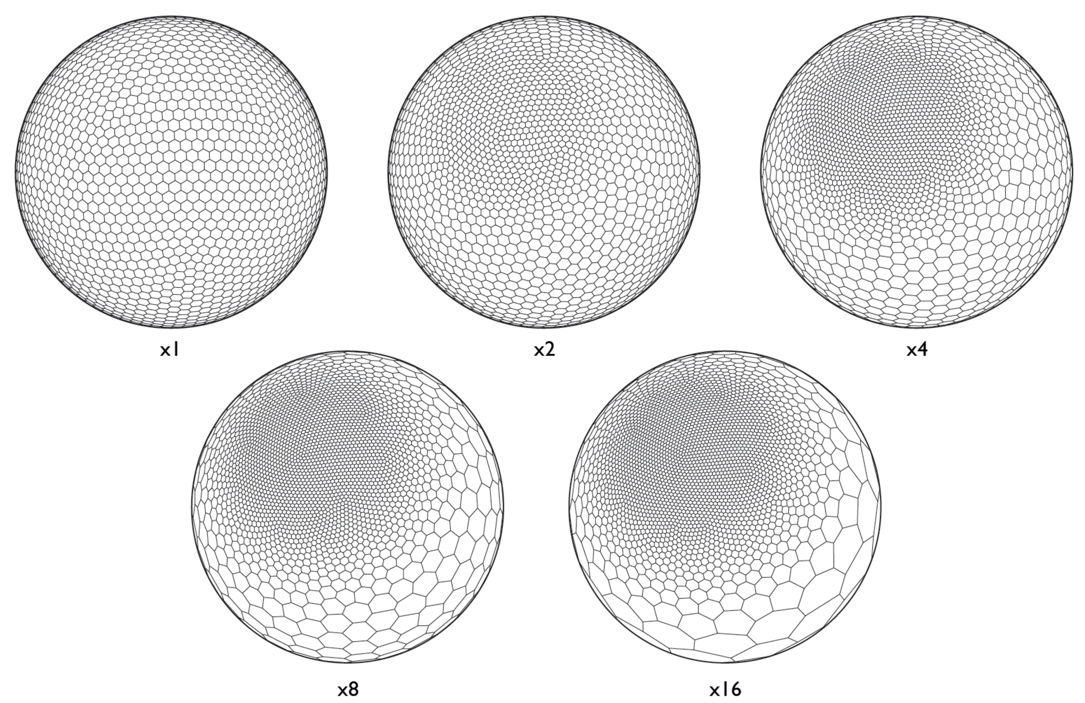

Figure 1: MPAS global grid with increasing regional refinement. The first figure shows a quasi-uniform grid and the subsequent figures show increasing resolution in a fixed region of the domain. Each grid has the same number of cells.

- The MPAS grid consist of cell center, cell vertex and cell edge points (see figure 2). The cell centers are at the centroid of the cell.
- In general the grid consists of polygonal cells with edge number ≥ 4. Most but not all cells are hexagonal for non-quadrilateral grids.
- MPAS-seaice uses an Arakawa 'B' grid with velocity components collocated at cell vertices. A locally cartesian grid is defined at each vertex which specifies the velocity directions.
- MPAS-seaice can use conventional quadrilateral grids.
- The velocity solver of MPAS-seaice reduces to that of CICE when quadrilateral grids are used.

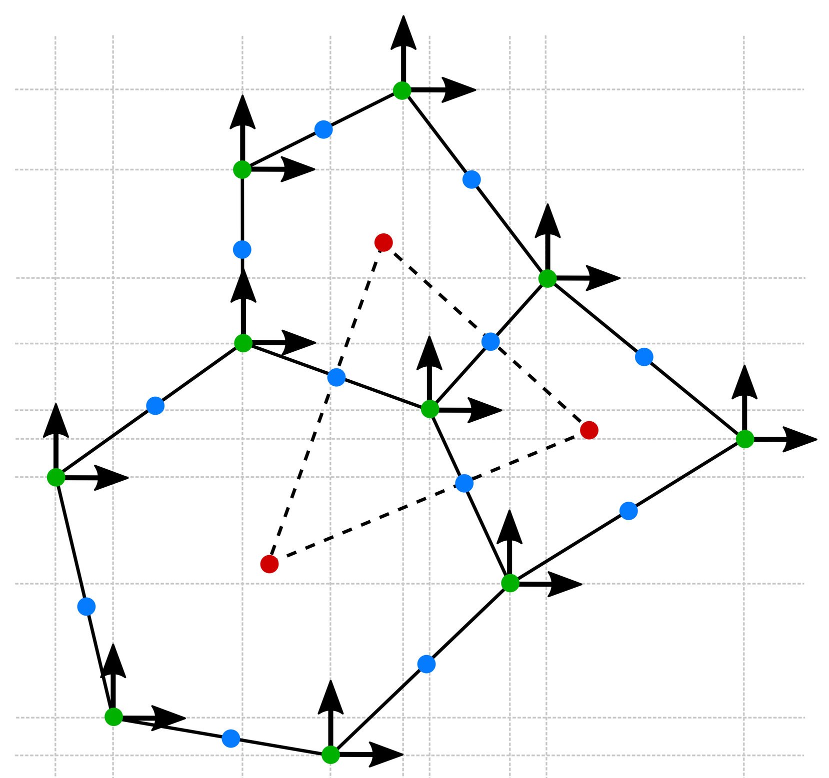

Figure 2: Detail of part of a MPAS grid. The grid consists of three types of points: (*red*): cell centers, (*green*): cell vertices, and (*blue*): cell edges. The cell centers also form a dual triangular mesh (*dashed black lines*). MPAS-seaice uses an Arakawa 'B' grid with u and v velocities collocated at cell vertices. The velocity directions are defined by a locally cartesian grid (*dashed grey lines*).

Velocity solver

- The velocity solver of MPAS-seaice is a generalization of that used by CICE [2, 3]. The generalization allows the velocity solver to use arbitrary shaped polygonal cells instead of being restricted to quadrilateral cells.
- The velocity solver solves the sea-ice momentum equation in an identical way to CICE except it uses more general basis functions for discretizing the internal stress term.
- The internal stress term uses a variational principle to determine the divergence of stress operator that forms the internal stress term.
- The derivation of the internal stress is based on fact that over the entire domain, ignoring boundary effects, the total work done by the internal stress is equal to the dissipation of mechanical energy:

$$\int_\Omega v.(\nabla \cdot \sigma)\mathrm{d}A = -\int_\Omega (\sigma_{11}\dot{\epsilon}_{11} + \sigma_{22}\dot{\epsilon}_{22} + 2\sigma_{12}\dot{\epsilon}_{12})\mathrm{d}A.$$

- The integral is performed by using basis functions to define velocity, stress and strain across each cell. Wachspress basis functions are used for the polygonal cells (see figure 3).

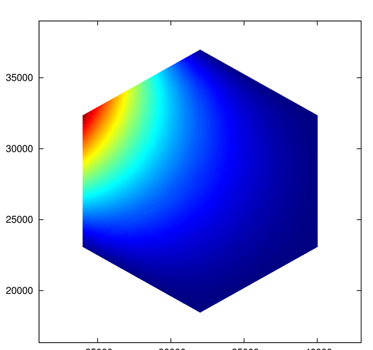

Figure 3: Wachspress basis function on a regular hexagonal cell. The function is 1 at the chosen vertex and zero at the others.

- The variation of the integral with respect to the velocity at a vertex point is taken. This gives the divergence of stress operator $(\nabla \cdot \sigma)$.
- The model must perform geometrical numerical integrations over each cell of the form

$$\mathcal{S}^x_{ij} = \int \mathcal{W}_i \frac{\partial \mathcal{W}_j}{\partial x}\mathrm{d}x\mathrm{d}y, \quad \mathcal{S}^y_{ij} = \int \mathcal{W}_i \frac{\partial \mathcal{W}_j}{\partial y}\mathrm{d}x\mathrm{d}y, \quad \mathcal{T}_{ij} = \int \mathcal{W}_i\mathcal{W}_j\mathrm{d}x\mathrm{d}y$$

at initialization, where $\mathcal{W}_i$ is the Wachspress basis function for vertex i of the polygonal cell.
- The velocity solver has been tested with an 80 km by 80km square planar domain test case [4].
- In the test case the sea ice has constant thickness of 2m and the concentration increases across the domain in the x direction from 0 to 1.
- Applied wind and ocean current fields are as shown in figure 4.

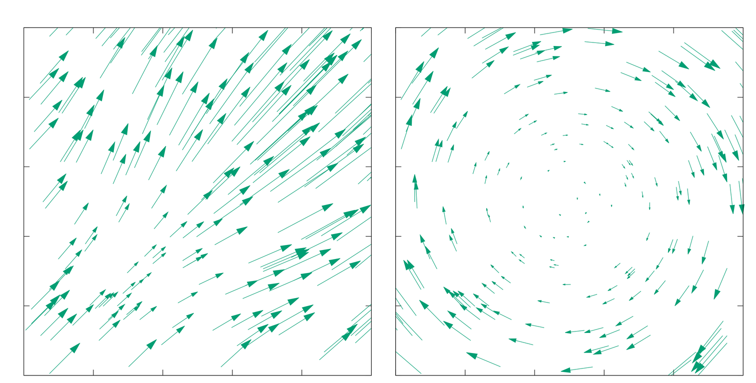

Figure 4: (*left*): Applied wind field for the square test case. Wind speed varies between 4 and 10 m/s. (*right*): Applied ocean current field for the square test case. Current speed varies from 0 to 0.14 m/s.

- Velocity solver results from MPAS-seaice have been compared to those of CICE. Both quadrilateral and hexagonal grids show near identical results between MPAS-seaice and CICE for velocity (see figure 5) and divergence of stress (see figure 6).

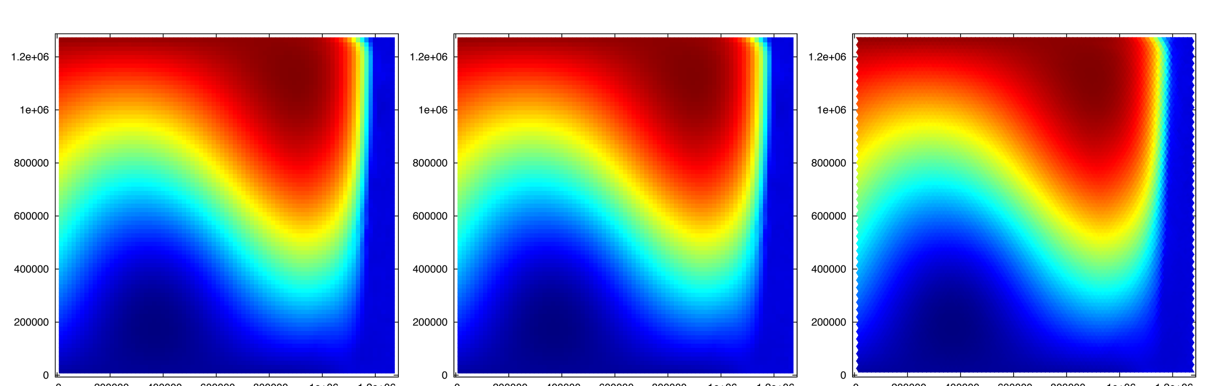

Figure 5: u (rightwards) sea-ice velocity component for an 80 km by 80km planar square test case. Ice concentration increases from 0 to 1 from left to right in the domain, with constant 2m ice thickness. (*left*): CICE. (*middle*): MPAS-seaice for the same quadrilateral grid as CICE. (*right*): MPAS-seaice on a regular hexagonal grid.

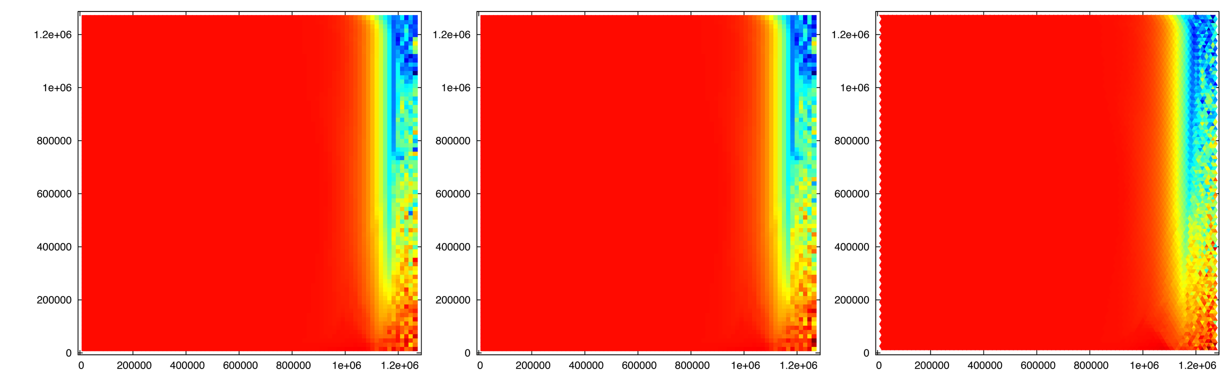

Figure 6: u component of the divergence of stress for the same test case as figure 5. (*left*): CICE. (*middle*): MPAS-seaice for the same quadrilateral grid as CICE. (*right*): MPAS-seaice on regular hexagonal grid.

- The yield curves for MPAS-seaice and CICE are also near identical (see figure 7).

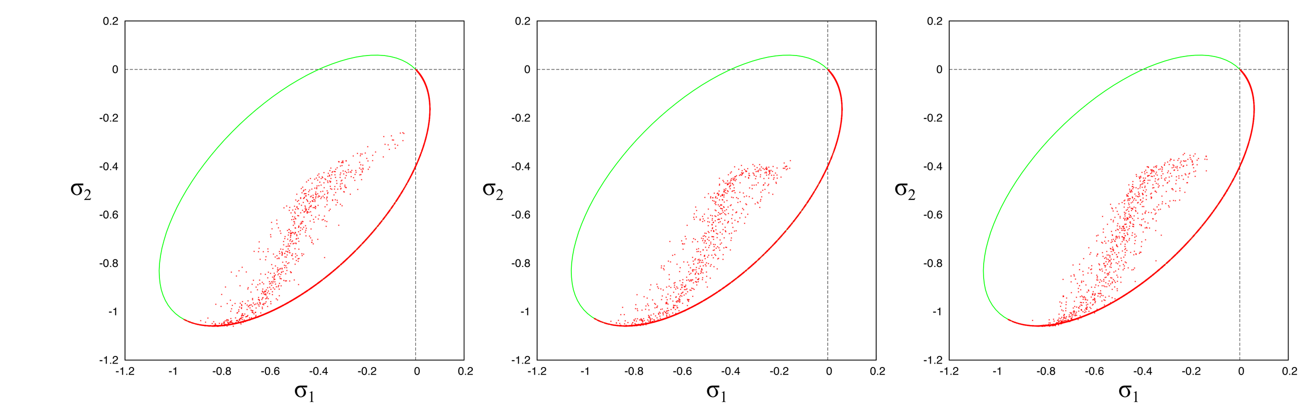

Figure 7: Yield curve for same test case as figure 5. (*left*): CICE. (*middle*): MPAS-seaice for the same quadrilateral grid as CICE. (*right*): MPAS-seaice on regular hexagonal grid.

Advection

- MPAS-seaice uses incremental remapping for its advection algorithm [5].
- Vertex velocities are used to trace back through time the cell vertices to estimate the position of the cell boundaries at the previous time step (see figure 8). This previous cell position is called the departure region.
- A linear reconstruction of the previous time step tracer field is integrated over the departure region to determine the tracer value at the next time step.
- The method is second order accurate and efficient for large numbers of tracers.
- It has been extensively tested and displays low numerical diffusion (see figure 9)

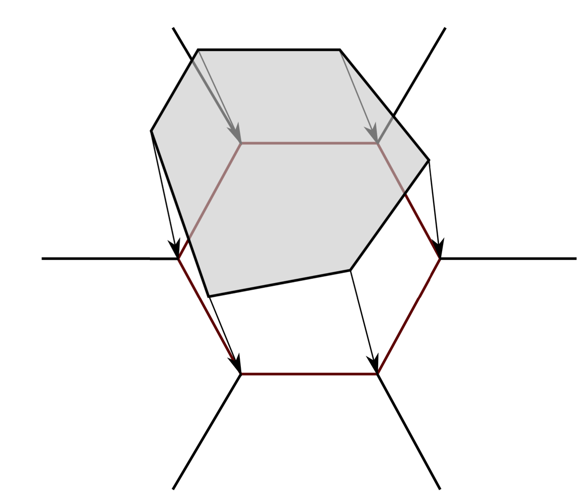

Figure 8: The departure region for a hexagonal cell during incremental remapping.

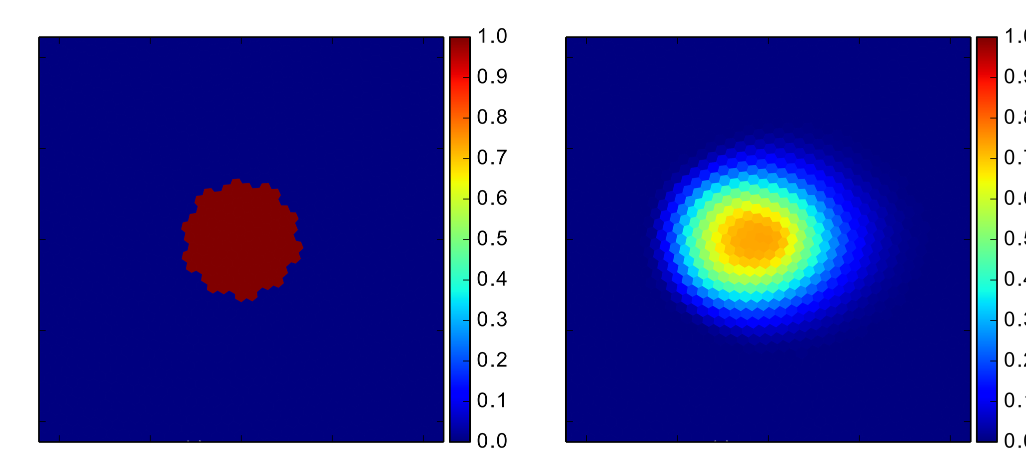

Figure 9: Sea ice concentration during advection of a disk of sea ice (radius of 10% of the Earth's radius) by a constant uniform 1m/s velocity field using the MPAS-seaice incremental remapping routine. (*left*): Uniform disk before advection. (*right*): Same disk of sea ice after being advected for exactly one circumnavigation of the Earth.

Column physics

- MPAS-seaice uses the same column physics (shortwave radiation, ice thickness distribution, vertical thermodynamics and mechanical redistribution) as CICE.
- The column physics in CICE has been placed in a modular "column physics package" library. Both MPAS-seaice and CICE use the same code.

Realistic simulations

- An atmosphere and ocean forcing module has been written to allow realistic global simulations.
- The model is in the process of being tested with increasingly high resolution realistic global simulations (see figure 10).
- Analysis modules have been written to allow most common diagnostics to be calculated at run time.

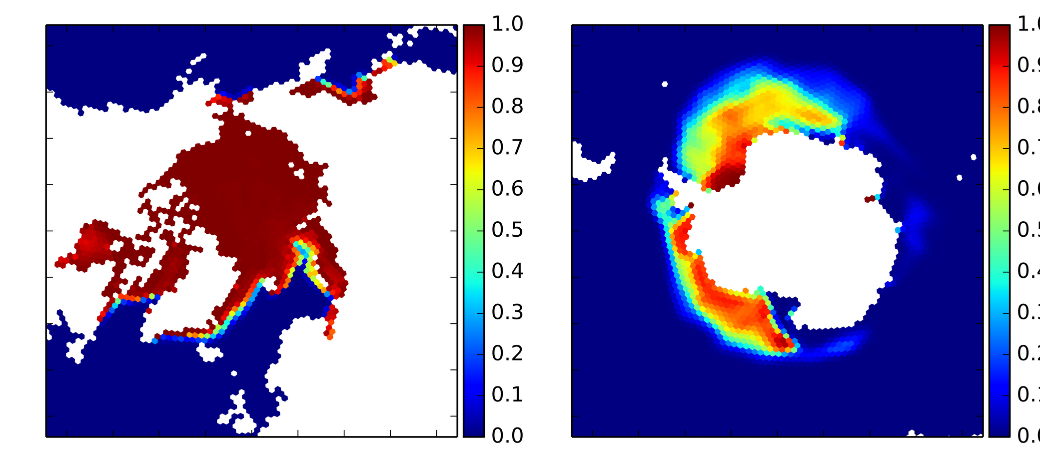

Figure 10: Sea ice concentration in January after one year of realistically forced simulations using the quasi-uniform 120km grid. (*left*): Arctic region. (*right*): Antarctic region.

Future work

- MPAS-seaice is being coupled into the Department of Energy's new global climate model, the Accelerated Climate Model for Energy (ACME) [6].
- Fully coupled global climate simulations will begin next year with ACME.
- The model will be tested on variable resolution grids shortly.
- New grid partitions are being developed for improved performance (see figure 11). MPAS allows very flexible grid partition between processors.

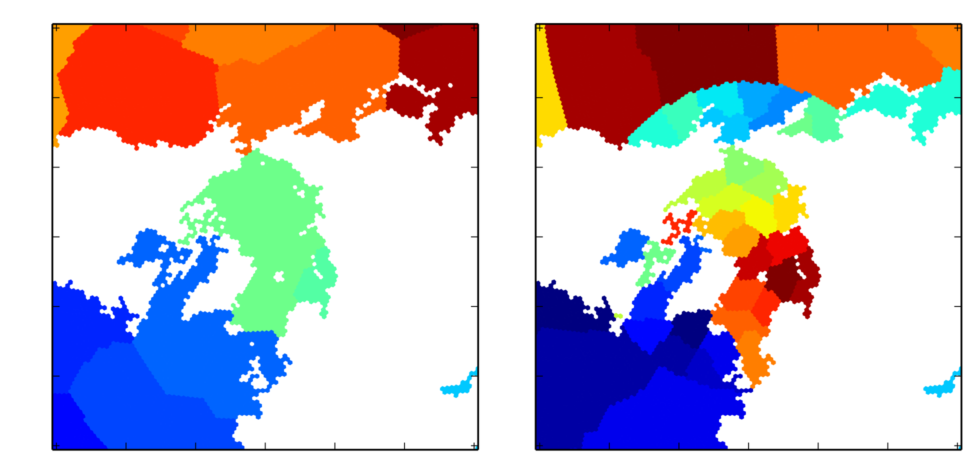

Figure 11: (*left*): Standard MPAS grid partition for 32 processors for a quasi-uniform 120 km global grid. Each color represents grid cells owned by a single processor. This grid would have poor load balancing because most of the Arctic sea-ice is on a single processor. (*right*): Improved grid partition for 32 processors with Arctic sea-ice more evenly shared amongst the 32 processors.

References

[1] T. Ringler, M. Petersen, R. L. Higdon, D. Jacobsen, P. W. Jones, M. Maltrud, A multi-resolution approach to global ocean modeling, *Ocean modeling*, **69** (2013)

[2] E. C. Hunke, J. K. Dukowicz, An elastic-viscous-plastic model for sea ice dynamics, *Journal of Physical Oceanography*, **27**, 1849–1867 (1997)

[3] E. C. Hunke, J. K. Dukowicz, The elastic-viscous-plastic sea ice dynamics model in a general orthogonal curvilinear coordinates on a sphere – incorporation of metric terms, *Monthly Weather Review*, **130**, 1848–1865 (2002)

[4] E. C. Hunke, Viscous-plastic sea ice dynamics with the EVP model: linearization issues, *Journal of Computational Physics*, **170**, 18-38 (2001)

[5] W. H. Lipscomb, E. C. Hunke, Modeling sea ice transport using incremental remapping, *Monthly Weather Review*, **132**, 1341–1354 (2004)

[6] http://climatemodeling.science.energy.gov/projects/accelerated-climate-modeling-energy